Tumors induce a subset of inflammatory monocytes with immunosuppressive activity on CD8+ T cells

Giovanna Gallina,[1] Luigi Dolcetti,[1] Paolo Serafini,[2] Carmela De Santo,[1] Ilaria Marigo,[1] Mario P. Colombo,[3] Giuseppe Basso,[4] Frank Brombacher,[5] Ivan Borrello,[2] Paola Zanovello,[1,6] Silvio Bicciato,[7] and Vincenzo Bronte[1]

[1]Istituto Oncologico Veneto, Padua, Italy. [2]Sidney Kimmel Comprehensive Cancer Center at Johns Hopkins, Baltimore, Maryland, USA. [3]Immunotherapy and Gene Therapy Unit, Department of Experimental Oncology, Istituto Nazionale Tumori, Milan, Italy. [4]Department of Pediatrics, University of Padua, Padua, Italy. [5]Institute for Infectious Diseases and Molecular Medicine, University of Cape Town, Cape Town, South Africa. [6]Department of Oncology and Surgical Sciences, Oncology Section, and [7]Department of Chemical Engineering Processes, University of Padua, Padua, Italy.

Active suppression of tumor-specific T lymphocytes can limit the efficacy of immune surveillance and immunotherapy. While tumor-recruited CD11b+ myeloid cells are known mediators of tumor-associated immune dysfunction, the true nature of these suppressive cells and the fine biochemical pathways governing their immunosuppressive activity remain elusive. Here we describe a population of circulating CD11b+IL-4 receptor α+ (CD11b+IL-4Rα+), inflammatory-type monocytes that is elicited by growing tumors and activated by IFN-γ released from T lymphocytes. CD11b+IL-4Rα+ cells produced IL-13 and IFN-γ and integrated the downstream signals of these cytokines to trigger the molecular pathways suppressing antigen-activated CD8+ T lymphocytes. Analogous immunosuppressive circuits were active in CD11b+ cells present within the tumor microenvironment. These suppressor cells challenge the current idea that tumor-conditioned immunosuppressive monocytes/macrophages are alternatively activated. Moreover, our data show how the inflammatory response elicited by tumors had detrimental effects on the adaptive immune system and suggest novel approaches for the treatment of tumor-induced immune dysfunctions.

Introduction

Tumor development is often accompanied by a peculiar alteration of hematopoiesis that leads to a progressive accumulation of myeloid cells in bone marrow, blood, and spleen and at the tumor site (1–5). These cells share the markers CD11b and Gr-1 (Ly6C/G), and their accrual correlates with the induction of T lymphocyte unresponsiveness to antigenic stimulation both in vitro and in vivo. CD11b+Gr-1+ cells inhibit antigen-activated T cells through a mechanism independent from a direct antigen presentation via MHC molecules (1–3, 6). The abnormalities of the immune response in tumor-bearing hosts can be corrected either by resection of the primary tumor, which results in a rapid normalization of the number of CD11b+Gr-1+ cells (7, 8), or by treatments affecting the magnitude and/or function of this population (9–11). These cells were named myeloid suppressor cells (MSCs; reviewed in ref. 12) on the basis of their functional inhibitory properties, since it has been difficult to define a distinct phenotype associated with the immunoregulatory activity. Indeed, CD11b+Gr-1+ cells are both heterogeneous and somewhat undifferentiated, since they include immature myelomonocytic cells, terminally differentiated monocytes, and granulocytes and can give rise to dendritic cells and macrophages as well as endothelial cells when exposed to appropriate signals or when residing in the proper microenvironment (1, 2, 5, 13–15).

Tumors release soluble factors (i.e., the cytokines GM-CSF, G-CSF, and IL-3) that contribute to MSC recruitment by enhancing myelopoiesis in the bone marrow and other hematopoietic organs such as the spleen in mice (12). On the other hand, tumor-derived factors also influence the differentiation of myelomonocytic precursors. For example, VEGF, M-CSF, and IL-6 were shown to inhibit differentiation of immature MSCs to dendritic cells, possibly through a mechanism requiring an activation of the STAT3 signal transduction pathway (16, 17). It appears that some cytokines are sufficient to elicit the expansion of MSCs and activate their immunoregulatory potential. GM-CSF is produced by many human and mouse tumor cell lines (2, 18–20), and a short course of recombinant GM-CSF administration is sufficient to cause MSC mobilization and temporary T cell unresponsiveness in immunocompetent mice (2).

Despite the uncertainties about the phenotype of MSCs, recent findings indicate that a common molecular mechanism seems responsible for the suppression of T cell activation. The metabolism of the amino acid L-arginine in MSCs is, in fact, critical for the control of T cell activation (21). In MSCs, L-arginine is metabolized mainly by arginase 1 (Arg1) and nitric oxide synthase 2 (Nos2) (21). Arg1 hydrolyzes L-arginine to urea and ornithine, whereas Nos2 oxidizes L-arginine to citrulline and NO. Nos2 and Arg1 can be used by MSCs separately or synergistically (21). Activation of either enzyme alone inhibits T cell proliferation by interfering with intracellular signal transduction pathways. Induction of both enzymes generates reactive nitrogen oxide species (such as peroxynitrites) under conditions of limited L-arginine availability, causing activated T cells to undergo apoptosis (22, 23). Either peroxynitrite scavengers or the com-
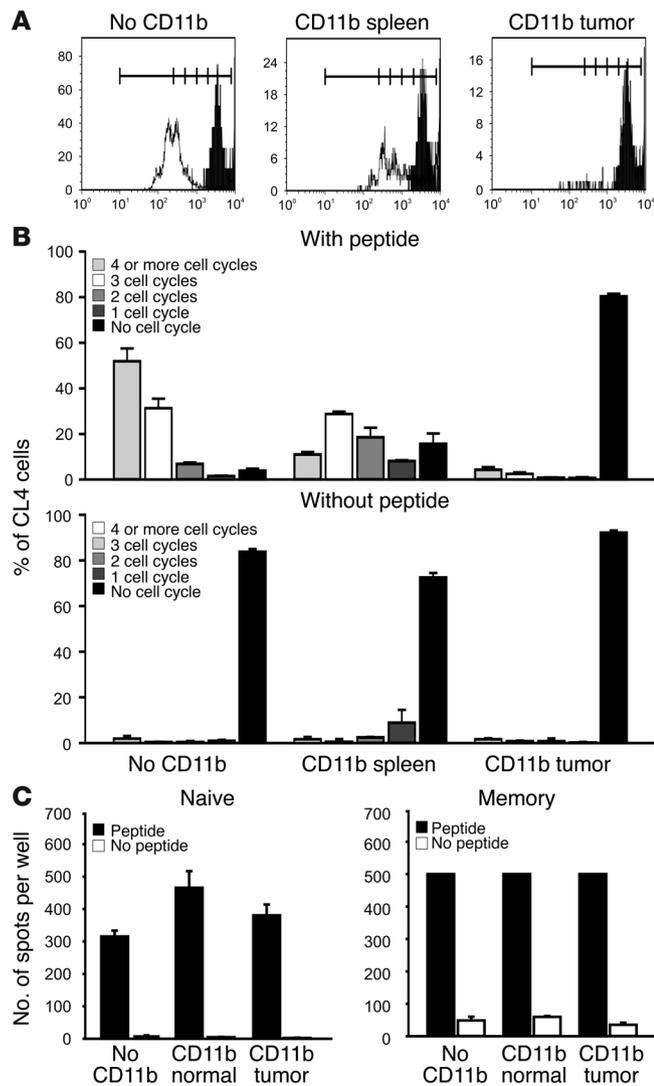

Figure 1

MSCs inhibit antigen-induced T lymphocyte proliferation but not IFN-γ release. (**A**) CFSE-labeled splenocytes derived from mice transferred with HA-specific CD8+ (CL4) T cells and primed with HA-encoding vaccinia virus were stimulated with the HA peptide in the absence (No CD11b) or in the presence of CD11b+ cells magnetically purified from either the spleen or the tumor infiltrate of tumor-bearing mice and admixed at a 1:10 ratio. The cultures were stimulated for 60 hours with the relevant peptide, and the clonotypic proliferation was evaluated as CFSE dilution by flow cytometry. (**B**) Data are presented as the mean percentage of CL4 cells in each cycle from triplicate wells (± SEM); 1 of 2 representative experiments is reported. (**C**) MSCs do not suppress IFN-γ production from naive or antigen-experienced (memory) CD8+ T cells. MSCs were isolated from the spleens of normal or tumor-bearing mice, and 6×10^5 cells were admixed with 3×10^6 splenocytes containing naive (2.4×10^5) or in vivo antigen-experienced (2.1×10^5) HA-specific CD8+ T cells stimulated with the relevant peptide in an ELISPOT assay. Data (mean ± SEM) are derived from triplicate wells of 1 representative experiment.

central elements of the delayed-type hypersensitivity response leading to microbicidal activity and cellular immunity, whereas alternatively activated macrophages are essential for humoral immunity, tissue repair, and allergic and antiparasitic responses (25).

In this manuscript we address some key aspects of MSC biology, define the phenotype of immunosuppressive MSCs as a subset of inflammatory monocytes, and explain how Th1 and Th2 cytokines collaborate in MSCs to activate a powerful metabolic pathway with negative consequences for the adaptive immune response of CD8+ T cells. Specifically, we show that IFN-γ production by antigen-activated T cells is required to arm MSCs, which are then able to integrate the signals from IFN-γ and IL-13 that they release. MSCs do not fit the strict separation between classic and alternatively activated macrophages, and they challenge the current idea that tumor-induced suppressor macrophages are alternatively activated (26).

Results

Functional properties of tumor-induced CD11b+ myeloid cells. In our studies we used initially the C26 colon carcinoma transduced to release mouse GM-CSF (C26-GM). The amount of GM-CSF produced by the C26-GM cell line was within the range of production by human and mouse tumor cell lines (22). Once inoculated s.c., C26-GM induced the rapid mobilization of myelomonocytic cells in the blood and spleen, and, 9 days after s.c. implantation, the spleen contained 2 main CD11b+ subsets, one expressing only CD11b and the other positive for both CD11b and Gr-1 antigens (22). Both fractions possessed suppressive activity on antigen-activated CD8+ T lymphocytes, whereas CD11b+ cells from tumor-free mice were not suppressive (see Supplemental Figure 1; supplemental material available online with this article; doi:10.1172/JCI28828DS1).

CD11b+ cells purified from the spleens of tumor-bearing mice were added as third party to CD8+ T lymphocytes (CL4 cells) expressing a transgenic TCR specific for the influenza HA. These lymphocytes had been primed in vivo with a vaccinia virus encoding HA and labeled with CFSE before culture to monitor cell division. The cultures were stimulated for 60 hours with the HA-derived immunodominant peptide, and clonotypic proliferation was evaluated as CFSE dilution by flow cytometry (Figure 1A). Dividing cells were plotted as a fraction of the total clonotypic CL4 cells (Figure 1B). In the presence of cognate peptide, CL4 cells underwent more than 4 divisions, whereas tumor-induced CD11b+ splenocytes reduced

bination of Arg and Nos inhibitors can block the immunosuppressive activity of MSCs and fully restore T cell responsiveness to antigen, in mouse tumor models as well as during chronic infection with the helminths (10, 14, 22, 24).

Despite the many advances recently achieved in understanding MSC physiology, some important issues still need to be addressed. Specifically, the nature of the immunoregulatory cell populations using the Arg/Nos pathways remains poorly defined. Moreover, it is very difficult to understand how Nos and Arg can be active in the same cell types, since these enzymes are antithetically regulated. Indeed, L-arginine metabolism in macrophages has been used as a parameter to discriminate between classically activated macrophages and alternatively activated macrophages (25). The Th1 cytokine IFN-γ, which drives the classic pathway of macrophage activation, enhances the activity of Nos2 to produce NO and inhibit Arg1 expression. Alternative activation is regulated by Th2 cytokines such as IL-4 and IL-13, which inhibit NOS2 activity and induce ARG1 synthesis. The existence of the reciprocal control of these enzyme activities in a cytokine-dependent manner has been taken as proof of distinct transition stages of macrophage life. Classically activated macrophages release proinflammatory cytokines and are

Table 1

Transcripts upregulated in CD11b+ splenocytes sorted from the spleens of tumor-bearing mice[A]

Gene name	Gene symbol	Accession number[B]	Fold change
Freshly isolated CD11b+ splenocytes			
Inflammatory-granulocyte response			
Regenerating islet–derived 3α	Reg3a	19694	147.70
Regenerating islet–derived 2	Reg2	19693	141.25
Amylase 1, salivary	Amy1	11722	124.54
Ribonuclease, RNase A family, 1 (pancreatic)	Rnase1	19752	100.93
Pancreatitis-associated protein	Pap	18489	73.81
Amylase 2, pancreatic	Amy2	11723	72.65
Regenerating islet–derived 3γ	Reg3g	19695	47.64
Pancreatic lipase-related protein 1	Pnliprp1	18946	40.48
Protease, serine, 2	Prss2	22072	39.62
Trypsin 4	Try4	22074	23.74
Kallikrein 5	Klk5	16622	19.91
Myeloperoxidase	Mpo	17523	19.81
Regenerating islet–derived 1	Reg1	19692	19.71
Chymotrypsinogen B1	Ctrb1	66473	16.28
Chymotrypsin-like	Ctrl	109660	14.3
Colipase, pancreatic	Clps	109791	14.04
Kallikrein 6	Klk6	16612	12.13
Chemokine (C-X-C motif) ligand 1	Cxcl1	14825	11.29
Eosinophil-associated, ribonuclease A family, member 2	Ear2	13587	7.84
TNF receptor–associated factor 1	Traf1	22029	7.81
Proteinase 3	Prtn3	19152	6.7
Fas (TNF receptor superfamily member)	Fas	14102	6.56
Kallikrein 22	Klk22	13646	6.25
Kallikrein 1	Klk1	16623	6.10
Eosinophil-associated, ribonuclease A family, member 1	Ear1	13586	5.23
Formyl peptide receptor 1	Fpr1	14293	4.12
Chemokine (C-X-C motif) ligand 2	Cxcl2	20310	3.78
Colony-stimulating factor 3 (granulocyte)	Csf3	12985	3.5
Chemokine (C-X-C motif) ligand 3	Ccl3	20302	3.15
Matrix metalloproteinase 8	Mmp8	17394	2.62
Elastase 2	Ela2	13706	2.46
Alternative macrophage activation signature			
IL-1 receptor, type II	Il1r2	16178	12.17
IL-10	Il10	16153	6.66
Mannose receptor, C type 1	Mrc1	17533	6.66
IL-1α	Il1a	16175	5.01
Chitinase 3–like 3	Chi3l3	12655	4.57
IL-6	Il6	16193	3.63
TGF-β–induced transcript 4	Tgfb1i4	21807	3.37
Adenosine A2b receptor	Adora2b	11541	3.26
Complement component 4	C4	12268	2.96
CD11b+ splenocytes cultured for 24 hours			
IL-4/IL-13 signature			
Arginase 1, liver	Arg	11846	142.18
IL-4–induced 1	Il4il	14204	26.24
Matrix metalloproteinase 12	Mmp12	17381	9.01
Annexin A4	Anxa4	11746	3.43
Serum/glucocorticoid–regulated kinase	Sgk	20393	3.55
Lectin, galactoside-binding, soluble, 3–binding protein	Lgals3bp	19039	4.29
IFN signature			
IL-12a	Il12a	16159	29.65
Signal transducer and activator of transcription 1	Stat1	20846	13.75
IFN regulatory factor 7	Irf7	54123	7.41
IFN-activated gene 202B	Ifi202b	26388	6.3
Histocompatibility 2, T region locus 10	H2-T10	15024	5.77
IFN regulatory factor 1	Irf1	16362	5.74
Transporter 1, ATP-binding cassette, subfamily B (MDR/TAP)	Tap1	21354	5
Proteasome (prosome, macropain) 28 subunit, α	Psme1	19186	4.17
IFN (α and β) receptor 2	Ifnar2	15976	3.78
NO synthase 2, inducible, macrophage	Nos2	18126	3.67
ATP-binding cassette, subfamily A (ABC1), member 1	Abca1	11303	3.34
Histocompatibility 2, D region locus 1	H2-D1	14964	3.02
Proteasome subunit, β type 5	Psmb5	19173	2.69
Proteasome subunit, α 1	Psma1	26440	2.28

[A]The average fold changes were obtained by comparison of freshly isolated and 24-hour-cultured CD11b+ splenocytes from tumor-bearing mice with control CD11b+ splenocytes from tumor-free mice. [B]LocusLink accession number.

antigen-specific T cell division to 1–3 cycles (Figure 1B). Cell death and reduced cell recovery during the culture of CL4 T cells in the presence of tumor-conditioned CD11b+ splenocytes indicate that antigen-activated clonotypic T cells eventually underwent apoptosis (Supplemental Figure 2) as suggested by previous findings in various models where MSCs have been studied (1, 27).

In addition to examining the proliferative activity, we sought to determine the extent to which MSCs could impact early effector functions. Naive or memory CL4 T cells were cocultured with normal or tumor-induced CD11b+ splenocytes and stimulated with the HA-specific peptide. IFN-γ production was determined by ELISPOT. No change could be seen between normal and tumor-derived CD11b+ cells (Figure 1C); this is consistent with the fact that MSCs do not block the early events of T cell activation (28). As we show below, early events of lymphocyte activation likely deliver important signals favoring the maturation of CD11b+ cells into a fully suppressive phenotype.

Gene expression profiling of CD11b+ splenocytes. Use of different cell surface markers has not been sufficient to dissect further the heterogeneity of MSCs and to identify the cells endowed with the immunoregulatory properties. Therefore, we performed a genomewide profiling approach using Affymetrix GeneChips. The RNA was extracted from CD11b+ cells enriched from pooled spleens of normal mice (about 5–10 spleens), and CD11b+ cells isolated from the spleens of single C26-GM tumor–bearing mice. These were analyzed immediately (time 0) or after a 24-hour incubation in complete medium. In vitro incubation was
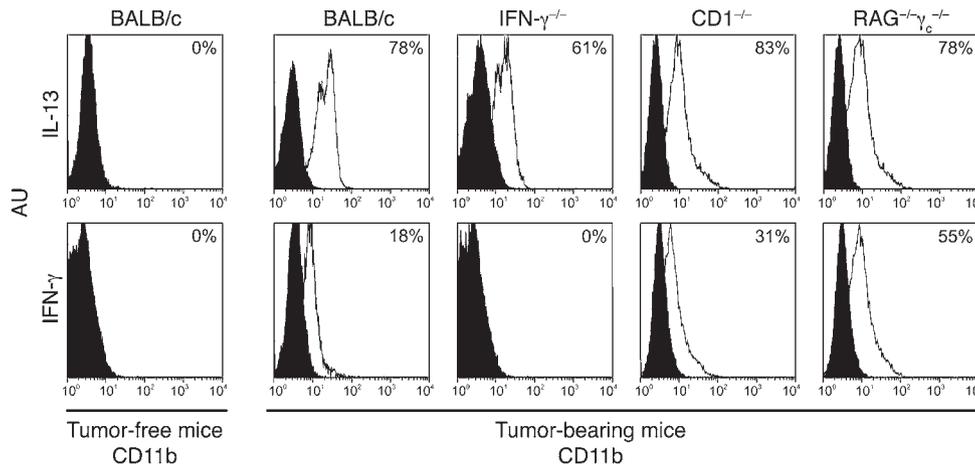
Figure 2
CD11b^{+} splenocytes from tumor-bearing mice produce both IFN-γ and IL-13. CD11b^{+} cells isolated from the spleens of normal BALB/c and different tumor-bearing mice (WT BALB/c, IFN-γ^{−/−}, CD1^{−/−}, and RAG^{−/−}γc^{−/−} KO mice) were analyzed by flow cytometry for intracellular presence of IL-13 (top panels) and IFN-γ (bottom panels). Open histograms indicate staining with IL-13 or IFN-γ antibody; filled histograms indicate staining with isotype-matched antibody controls. Data are representative of at least 3 determinations in separate experiments. MFI, mean fluorescence intensity (a log scale of 10^0–10^4 was used).

performed because we and others have shown that culture of MSCs increases their suppressive activity (1, 2, 5, 14), which suggests the existence of an internal differentiation/maturation program. Three biological mRNA replicates were hybridized for each group. The raw data have been deposited, and processed values and complete gene lists are available (Gene Expression Omnibus [GEO] accession no. GSE5455; http://www.ncbi.nlm.nih.gov/geo/).

Microarray analysis confirmed that the populations analyzed clustered in separate groups for a number of upregulated and downregulated genes (Supplemental Results, Supplemental Figures 3–5, and Supplemental Tables 2–8). CD11b^{+} splenocytes freshly isolated from tumor-bearing mice differed from the normal counterparts in regard to the presence of 2 main signatures. One identifies genes coding either for enzymes characterizing polymorphonuclear cells or for molecules associated with acute inflammatory responses (Table 1). The other signature comprises cytokines, membrane molecules, and markers associated with alternative activation of macrophages. This cluster included chitinase 3–like 3 (also known as Ym-1), complement component 4, IL-6, IL-10, IL-1α, IL-1 receptor II, TGF-β–induced transcript 4, and the C-type mannose receptor (25, 29). The A2b adenosine receptor is not unique for macrophages, since it is expressed in mast cells as well, but it has been associated with cytokine-induced macrophage deactivation (30). Taken together, these microarray data suggest that CD11b^{+} splenocytes comprise both inflammatory granulocytes and a subset of monocytes/macrophages. Other signatures could not be clearly associated with a peculiar cell type, and no clear marker of T, B, and NK lymphocytes was discernible (Supplemental Results and GEO accession no. GSE5455).

Comparison of CD11b^{+} splenocytes at time 0 and after 24 hours confirmed the existence of a cellular program leading to alternative macrophage activation. One of the most upregulated genes after 24 hours of culture, in fact, was *Arg1*, coding for the enzyme Arg1, which is a well-recognized marker of alternatively activated macrophages and also a critical enzyme for the inhibitory activ-

ity exerted by MSCs on activated T lymphocytes (21). Other genes were found to be spontaneously upregulated during the 24-hour culture that belong to the pathway activated by Th2-type cytokines such as IL-4 and IL-13 (Table 1). Accordingly, the mRNAs for most of these genes were upregulated by treatment of a cloned MSC population with IL-4 (Supplemental Table 9).

The program activated in CD11b^{+} splenocytes from tumor-bearing mice is more complex than a plain alternative activation, since many overexpressed genes are under the control of type I and type II IFNs. In particular, *Nos2* was also spontaneously upregulated (Table 1), which confirmed our previous findings of the unique, concomitant expression of both enzymes of L-arginine metabolism in tumor-induced CD11b^{+} splenocytes (10, 22). Taken together, these data indicate MSCs as a peculiar population that eludes the rigid classification of classically or alternatively activated macrophages and suggest the presence of MSC-released autocrine factors driving in vitro MSC maturation/differentiation.

CD11b^{+} splenocytes from tumor-bearing mice produce IFN-γ and IL-13 and require these cytokines to activate the suppressive program. We speculated that the gene expression profiles emerging after in vitro culture of tumor-induced CD11b^{+} splenocytes could result from the autocrine action of cytokines released by the same cells. IL-13 and IFN-γ were detectable in the supernatant of CD11b^{+} splenocytes isolated from tumor-bearing mice and cultured for 48 hours (160 ± 25 and 22,000 ± 235 pg/ml per 10^5 cells, respectively), and intracellular staining confirmed that a sizeable fraction of CD11b^{+} splenocytes from tumor-bearing but not from tumor-free mice produced both IFN-γ and IL-13 (Figure 2). Accordingly, CD11b^{+} splenocytes isolated from tumor-bearing IFN-γ KO mice produced IL-13, suggesting that expression of the 2 cytokines is uncoupled (Figure 2). IL-4 was not detected by ELISA, ELISPOT, or intracellular staining (data not shown).

To address further the role of Th1 and Th2 cytokines in the regulation of MSC function, we analyzed the in vitro generation of alloreactive CTLs in the presence of CD11b^{+} cells isolated from the spleens of tumor-bearing BALB/c mice, WT or deficient for either IFN-γ or IL-4. When tumor-induced CD11b^{+} cells were added to WT BALB/c lymphocytes stimulated with γ-irradiated C57BL/6 allogeneic cells, CTL generation was inhibited by either WT or IL-4 KO CD11b^{+} cells (Figure 3A). On the other hand, CD11b^{+} cells from IFN-γ KO mice were not suppressive but rather increased the number of alloantigen-specific CTLs recovered from the cultures. This indicates that the ability of CD11b^{+} cells to release IFN-γ but not IL-4 is important for the suppressive properties of tumor-induced CD11b^{+} cells. We then asked whether the release of cytokines from activated T cells could play a role in the suppressive pathways. Responder T cells from either IFN-γ KO (Figure 3B) or IL-4 KO (Figure 3C) mice were

A

B

C

LU$_{30}$ (% of control)
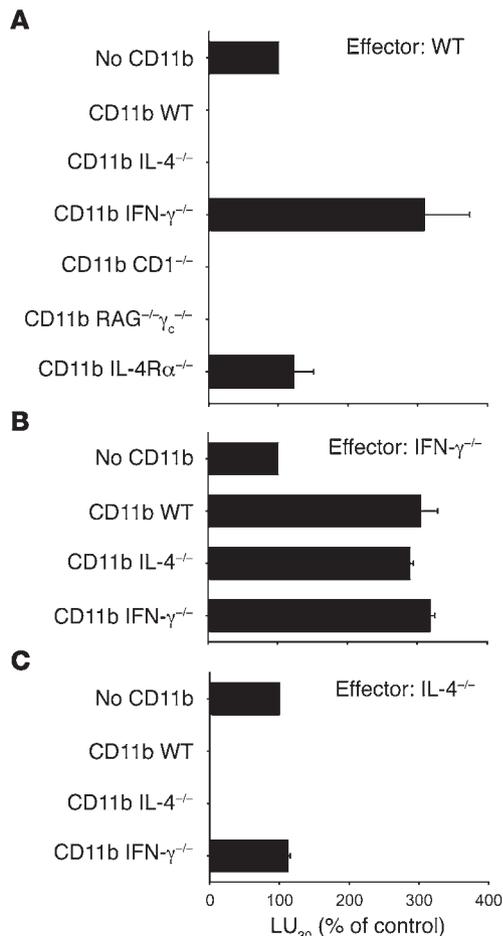
Figure 3
Evaluation of cytokines and cytokine receptors required by tumor-induced CD11b$^+$ cells to inhibit generation of alloreactive and tumor-specific CTLs. CD11b$^+$ sorted cells from tumor-bearing WT or different KO mice were added at a final concentration of 3% to a mixed leukocyte culture set up with BALB/c effectors stimulated with an equal number of C57BL/6 splenocytes. After 5 days, cytotoxic activity was tested in a 5-hour ^{51}Cr-release assay against either a syngeneic control target (CT26, H-2^d) or an allogeneic target (MBL-2, H-2^b). Effector lymphocytes were taken from WT (**A**), IFN-γ KO (**B**), or IL-4 KO (**C**) mice. LU$_{30}$, defined as the number of lymphocytes necessary to achieve 30% specific lysis of 2 × 10^3 target cells in a 5-hour assay, was calculated on the basis of the total number of viable cells recovered from the cultures. Data are expressed as the ratio between the LU$_{30}$ measured in cultures containing the third-party cells and in control cultures set up in the absence of third-party cells. Data are mean ± SEM from 3 experiments.

in addition to B and T lymphocytes (32). We also used CD1$^{-/-}$ mice to obtain CD11b$^+$ cells devoid of any contaminating NKT cells that might account for the IL-13 production. Berzofsky and colleagues, in fact, have shown that NKT cells releasing IL-13 can activate immunosuppressive CD11b$^+$Gr-1$^+$ cells in some mouse tumor models (9, 33).

Tumor-induced CD11b$^+$ cells from KO spleens had an intact suppressive activity on alloreactive CTLs (Figure 3A) and released IL-13 and IFN-γ as well as the WT counterparts (Figure 2). These data confirm that our results unveil a different pathway of suppression, not dependent on either NK or NKT cells. Moreover, since Rag2$^{-/-}$γ$_c^{-/-}$ KO mice are also deficient in T and B lymphocytes and lack the common γ chain that is a component of the type I IL-4R, we can conclude that (a) the immunosuppressive properties of CD11b$^+$ cells are a likely outcome of the direct activity of tumor-released factors on the myeloid precursors without requiring any additional intervention from cells of the innate or adaptive immune system; and (b) type I IL-4R, which binds only IL-4, does not play any role in the myeloid-dependent suppression. We can thus conclude that a successful suppression of CTL activity by tumor-induced CD11b$^+$ cells depends on the integration of signals coming from the IFN-γ, released both by activated T lymphocytes and from the same CD11b$^+$ cells, and IL-4Rα expressed on suppressor cells. These findings are further confirmed by the inability of IFN-γ$^{-/-}$ and IL-4Rα$^{-/-}$ CD11b$^+$ splenocytes of tumor-bearing mice to inhibit the proliferation of purified CD8$^+$ T cells stimulated with anti-CD3 and anti-CD28 mAbs (Supplemental Figure 1B).

The IFN-γ effect seems paradoxical in that CTLs produce IFN-γ, which in turn may act in trans to inhibit CTL function of other CTLs. To address further the role of this cytokine, we added either antibodies blocking IFN-γ or the recombinant cytokines to allo-cultures stimulated in the presence of either WT or IFN-γ KO MSCs (Supplemental Figure 6). These experimental data show that (a) inclusion of antibodies against mouse IFN-γ does not elevate dramatically the lytic response in normal allo-cultures devoid of MSCs, whereas it does restore completely immune responsiveness in cultures containing MSCs; and (b) exogenous IFN-γ can efficiently replace the cytokine produced by either T lymphocytes or MSCs (derived from either the spleen or tumor infiltrate) in sustaining T lymphocyte inhibition. The total amount of cytokine added to the culture to obtain this effect was rather high (50 ng/ml), in keeping with the notion that substantial and prolonged release of IFN-γ is necessary to exert the inhibitory effect on CTL activity.

CD11b$^+$IL-4Rα$^+$ cells constitute a subset of inflammatory monocytes able to produce IL-13 and IFN-γ. Having identified IL-4Rα as a possible MSC marker, we separated tumor-induced CD11b$^+$ spleno-

mixed with allogeneic targets in the presence of CD11b$^+$ cells from the different strains. Lack of IFN-γ production by alloantigen-stimulated T cells completely abrogated the suppressive activity, regardless of the origin of the tumor-induced CD11b$^+$ cells (Figure 3B). In contrast, the T cells' inability to produce IL-4 did not alter the suppression by third-party suppressors unless CD11b$^+$ cells from IFN-γ KO mice were used in the assay (Figure 3C). These results confirmed the requirement for IFN-γ production by both activated T lymphocytes and tumor-induced CD11b$^+$ cells and completely ruled out any contribution of IL-4 in CD11b$^+$-mediated suppression.

Having excluded IL-4, we considered the involvement of IL-13, since this cytokine plays a role in the alternative macrophage activation and induces ARG1 (25). We used mice deficient in the IL-4 receptor (IL-4R) α chain (CD124). The IL-4R is a heterodimeric complex composed of different chains. In the type I IL-4R, IL-4Rα and a common γ chain form a complex binding only IL-4, whereas the type 2 IL-4R is composed of IL-4Rα and IL-13R1 chains and binds both IL-4 and IL-13 (31). CD11b$^+$ cells were isolated from IL-4Rα KO tumor-bearing mice and added as a third party to the allo-cultures. The presence of IL-4Rα on CD11b$^+$ cells appeared to be critical for their suppressive activity (Figure 3A). Since IL-4 neither was released nor appeared involved in suppression, it is logical to assume that the receptor was activated by IL-13.

To exclude a possible role of contaminating NK cells as a source of IFN-γ among the sorted CD11b$^+$ splenocytes, we isolated CD11b$^+$ cells from the spleens of Rag2$^{-/-}$γ$_c^{-/-}$ KO mice, which lack NK cells
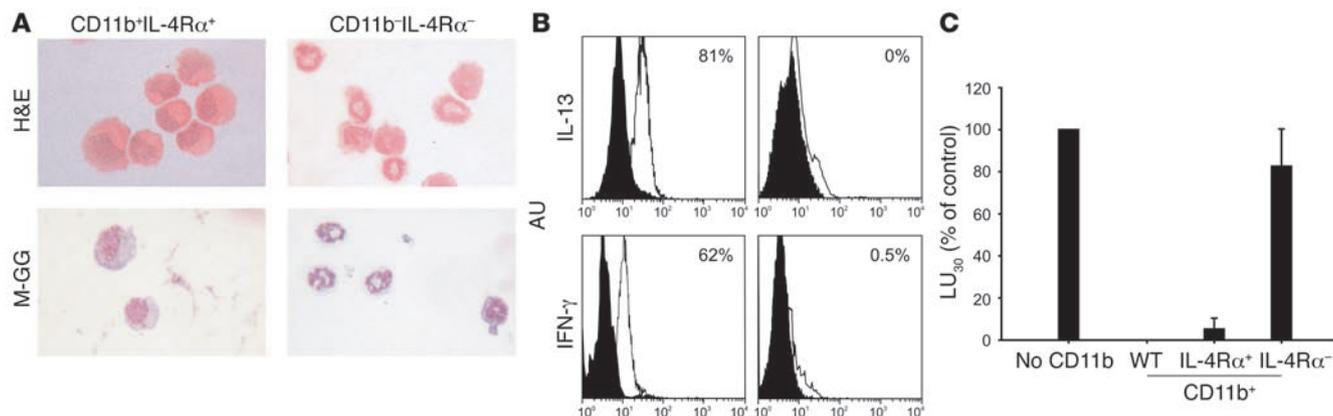
Figure 4
Morphological and functional characterization of tumor-induced CD11b+IL-4Rα+ and CD11b+IL-4Rα− cells. Splenocytes were sorted by micro-beads to select CD11b+ cells, and this cellular population was subsequently sorted by flow cytometry to select IL-4Rα+ (left panels) and IL-4Rα− (right panels) cells. (**A**) The sorted cells were stained with H&E and May-Grünwald-Giemsa stain (M-GG). Pictures were taken under microscopy at ×40 magnification. CD11b+IL-4Rα+ cells showed a monocytic morphology, while CD11b+IL-4Rα− cells comprised granulocytes at various differentiation stages, including immature cells with band morphology. (**B**) Both populations were analyzed by flow cytometry for their expression of IL-13 (top panels) and IFN-γ (bottom panels). Open histograms indicate staining with IL-13 or IFN-γ antibody; filled histograms indicate isotype-matched antibody control. Data are representative of at least 3 determinations in separate experiments. (**C**) The 2 populations were added at a final concentration of 3% to alloantigen-stimulated cultures (see above). CD11b+IL-4Rα+ but not CD11b+IL-4Rα− cells suppressed the generation of alloreactive CTLs ($P < 0.01$ and $P = 0.48$, respectively). Results are shown as the fraction of LU_{30} measured in the control allo-cultures lacking third-party CD11b+ cells. Data are mean ± SEM from 3 experiments.

cytes according to its expression. This procedure distinguished 2 subpopulations of CD11b+ cells, the monocytes (IL-4Rα+) and the polymorphonuclear cells (IL-4Rα−) (Figure 4A). With this approach, we could use a single cell surface marker to differentiate the 2 main signatures unveiled by microchip analysis. The IL-4Rα+ fraction also contained some cells with a more immature morphology consistent with myelomonocytic precursors. The IL-4Rα+ but not the IL-4Rα− sorted cells constitutively released IL-13 and IFN-γ and suppressed the generation of alloreactive CTLs (Figure 4, B and C), indicating that the expression of IL-4Rα can indeed be considered a marker of tumor-induced, circulating MSCs.

In mice bearing a 9-day-old s.c. C26-GM tumor, CD11b+IL-4Rα+ monocytes are present not only in the spleen but also in the blood, where they can constitute a large fraction of the total mononuclear cells (48.2% ± 6.52% in tumor-bearing versus 1.2% ± 0.68% in tumor-free mice). Circulating mouse monocytes comprise at least 2 distinct subpopulations: CD11b+Gr-1−CCR2−CX₃CR1high monocytes are precursors of resident macrophages in normal tissues, whereas CD11b+Gr-1+CCR2+CX₃CR1low cells are "inflammatory" monocytes that home to sites of inflammation, where they serve as a reservoir of dendritic cells and activated macrophages (34, 35). Flow cytometry analysis on sorted CD11b+ cells from tumor-bearing hosts indicates that the IL-4Rα+ splenocytes express a low level of CX₃CR1 and are positive for CCR2 and CD62L (Figure 5A). Moreover, about half of the CD11b+IL-4Rα+ monocytes are Gr-1+, bona fide inflammatory monocytes (Figure 5A). However, Gr-1+ and Gr-1− fractions might be part of the same continuum, since CD11b+Gr-1+ cells can differentiate in vitro and in vivo into CD11b–single positive cells (1, 2, 5, 14, 35).

To evaluate whether CD11b+IL-4Rα+ cells could be induced by unmanipulated tumors, we analyzed the blood and the spleen of mice bearing s.c. tumors known to induce systemic immune dysfunction (2, 5, 10, 14, 17). Tumors were allowed to grow until they

reached about 1 cm², and then pools of blood samples and spleens were stained. In all cases, blood and spleen contained various numbers of CD11b+IL-4Rα+ cells, whereas these cells were very few in the tumor-free BALB/c and C57BL/6 mice (Figure 5B).

Even though CT26, a colon carcinoma closely related to the C26 cell line from which the C26-GM tumor model was originated, did not induce high numbers of CD11b+ splenocytes, they were equally suppressive on a per-cell basis (Figure 5C), indicating that GM-CSF transduction was basically enhancing an innate property of the tumor cells. More importantly, CD11b+ cells in the spleens of CT26 tumor–bearing mice behaved as did the cells described previously, since they required the ability to produce IFN-γ and the expression of IL-4Rα in order to be immunosuppressive (Figure 5C). Similar results were obtained with the CD11b+ cells enriched from spleens of BALB/c mice bearing the mammary carcinoma 4T1 (Figure 5C).

Since some key KO mice were not available in the H-2b background, we used a different approach for MCA203 and EL-4 tumors growing in syngeneic C57BL/6 mice. We added mAbs blocking either IL-13 or IFN-γ antibodies to allo-cultures containing, as a third party, CD11b+ splenocytes from tumor-bearing mice. Whereas alloreactive T lymphocytes were generated in standard allo-cultures from tumor-free mice, there was a complete loss of this alloresponse in cultures receiving CD11b+ splenocytes conditioned by either MCA203 or EL-4 tumors. Active cytotoxic effectors could be recovered by addition of either anti–IFN-γ or anti–IL-13 mAbs but not a control mAb, which suggests that each cytokine had a key function in sustaining the suppressive response; moreover, the combination of blocking mAbs resulted in an additive/synergistic activity, since it allowed to double the number of alloreactive T lymphocytes recovered in the cultures (Figure 5C). Regardless of the tumor type and the mouse genetic background, these data indicate that the interplay between the antithetical cytokines IFN-γ and IL-13 (via IL-4Rα) underlies the immunosuppressive pathway.
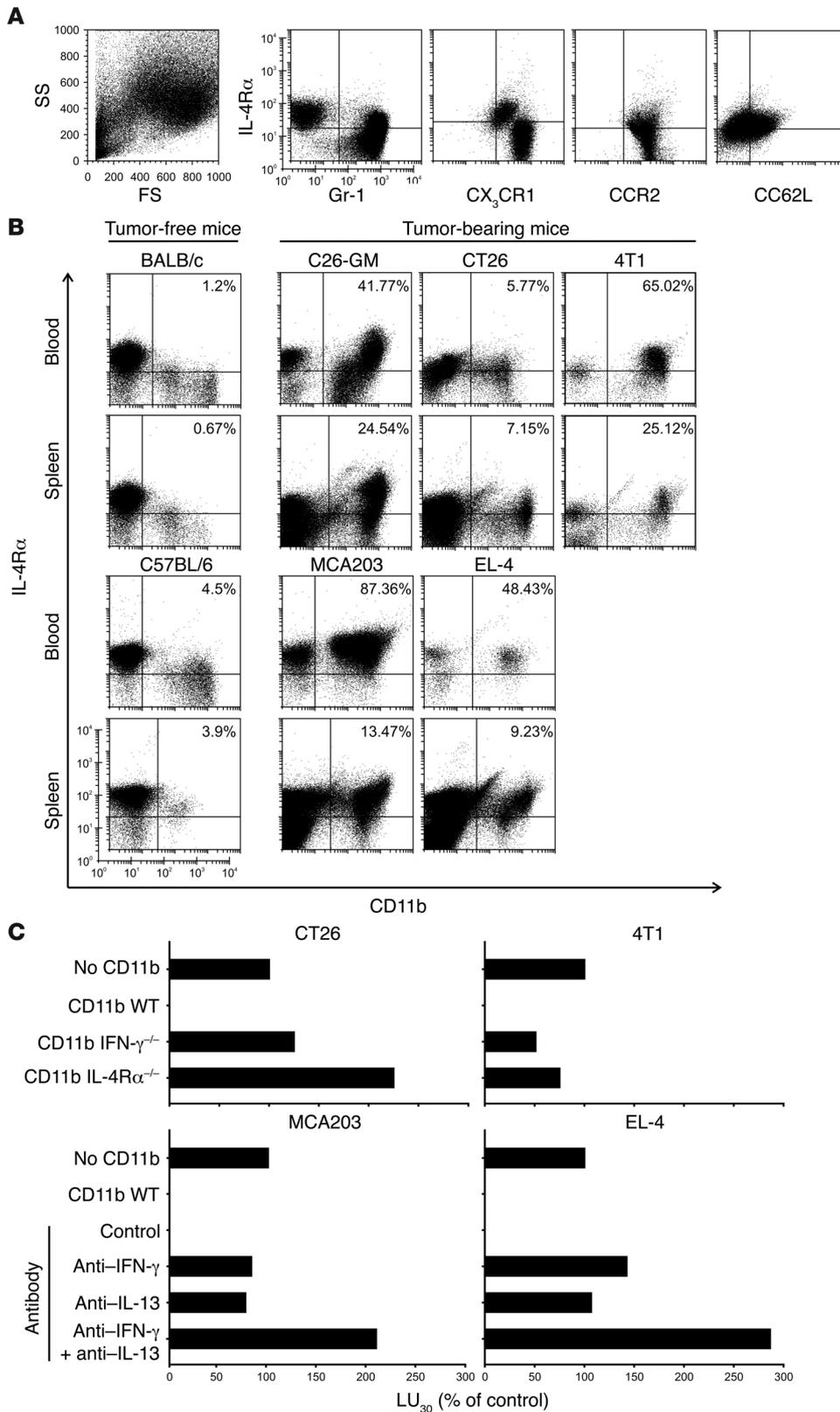
Figure 5
Phenotypic characterization of tumor-induced CD11b+IL-4Rα+ cells. (**A**) CD11b+ cells from spleens of mice inoculated 9 days earlier with C26-GM tumor cell lines were enriched through immuno-magnetic microbeads and stained with the indicated antibody. FS, forward scatter; SS, side scatter. (**B**) Blood cells (top rows) and spleen cells (bottom rows) from mice of various strains inoculated with different tumors were stained for CD11b and IL-4Rα. The following tumor cell lines were used: the BALB/c-derived colon carcinoma CT26 (closely related to the C26 tumor used in our previous experiments) and mammary carcinoma 4T1; and the C57BL/6–derived EL-4 lymphoma and MCA203 fibrosarcoma. Data are from a single experiment representative of 3. (**C**) CD11b+ cells were sorted from the spleens of tumor-bearing WT or KO BALB/c mice and added at a final concentration of 3% to a mixed leukocyte culture set up as previously described (top panels). CD11b+ cells sorted from the spleens of tumor-bearing C57BL/6 mice were added at a final concentration of 3% to a mixed leukocyte culture set up with C57BL/6 effectors stimulated with an equal number of γ-irradiated BALB/c splenocytes, in the presence or absence of anti–IFN-γ and/or anti–IL-13 mAbs added at the beginning and at the third day of culture (bottom panels).

IL-4Rα expression is required for the in vivo inhibitory activity of myeloid cells in tumor-bearing hosts. To prove that IL-4Rα is not just a cell marker but is critical for the function of suppressive myeloid cells, we inoculated s.c. C26-GM cells in LysM^CreIL-4R^−/flox mice that have a targeted knockout of the IL-4Rα in macrophages and neutrophils (36). Tumors grew similarly in IL-4Rα conditional
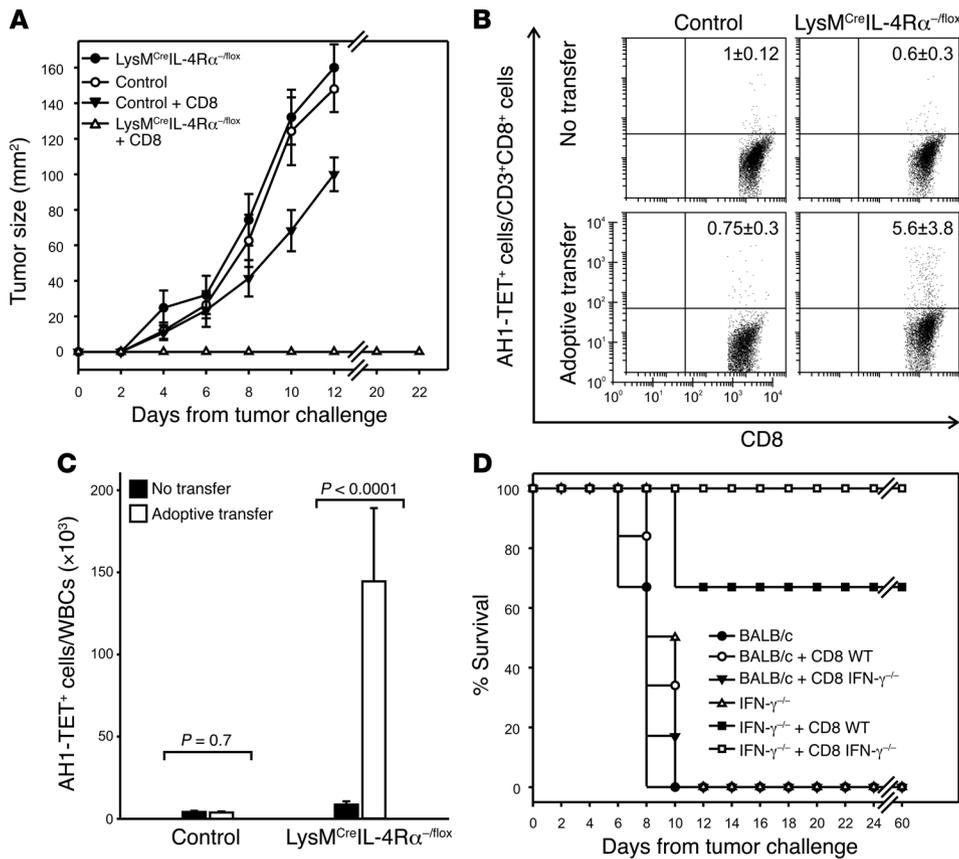
Figure 6
Adoptive cell transfer is effective only in mice with a myeloid-restricted inactivation of IL-4Rα. (**A**) LysM[Cre]IL-4R[−/flox] mice and control littermates were challenged s.c. on day 0 with C26-GM cells and were given, 24 hours later, CD8+ T cells purified from the spleens and lymph nodes of mice vaccinated 14 days before with γ-irradiated C26-GM cells. Tumor size is indicated as the product of the 2 main perpendicular diameters measured with a caliper. Mice with tumors had to be euthanized on day 12, since they were showing severe signs of distress. (**B**) The CD3+CD8+ cells positive for the L[d] tetramer loaded with AH1 peptide were determined in the blood of tumor-bearing mice 8 days after tumor inoculation. One dot plot for each group is reported. Numbers indicate the percentages of AH1-TET+ cells among gated CD3+CD8+ T lymphocytes (mean ± SEM, n = 5–6). (**C**) The absolute numbers of CD3+CD8+AH1-TET+ cells were calculated for the total number of circulating white blood cells (WBCs) and reported as mean ± SEM. The background staining given by control β-gal[876–884]/L[d] TET was subtracted for each determination. (**D**) IFN-γ^{−/−} and WT BALB/c mice were challenged s.c. on day 0 with C26-GM cells and given, 24 hours later, CD8+ T cells purified from the spleens and lymph nodes of IFN-γ^{−/−} and WT BALB/c mice, vaccinated 14 days before with γ-irradiated C26-GM cells. Results, expressed as survival rates after tumor challenge, are from 1 representative experiment with 6 mice per group.

blood cells in BALB/c mice (38). We transferred only 57,500 AH1-specific CD8+ T lymphocytes, and we calculated a total of 144,503 (± 44,579) AH1-TET+CD3+CD8+ T cells circulating in the blood of LysM[Cre]IL-4R[−/flox] tumor-bearing mice 8 days after adoptive transfer. These mathematical considerations indicate that tumor-specific T cells expanded in LysM[Cre]IL-4R[−/flox] tumor-bearing mice but not in control littermates (Figure 6C). Thus, tumor-specific CD8+ T lymphocytes are inhibited by C26-GM tumor growth in vivo, and this inhibition critically requires the expression of IL-4Rα in myeloid cells.

We also evaluated the importance of IFN-γ by adoptively transferring tumor-specific CD8+ T cells isolated from either WT or IFN-γ^{−/−} mice to WT or IFN-γ^{−/−} tumor-bearing mice (Figure 6D). In this way, we could evaluate the relevance of IFN-γ produced by antitumor T cells or by cells of the tumor-conditioned host. In agreement with the in vitro data, a full antitumor activity of adoptive immunotherapy could be obtained in the complete absence of IFN-γ, since the IFN-γ^{−/−} mice receiving IFN-γ^{−/−} CD8+ T cells were completely cured and survived for the entire observation period (Figure 6D; P = 0.001). Moreover, about 65% of IFN-γ^{−/−} mice bearing C26-GM were cured by transfer of WT CD8+ T cells (P = 0.008), suggesting that the endogenous production of IFN-γ is more relevant that the release of IFN-γ by effector lymphocytes in regulating tumor-induced suppression in vivo (Figure 6D).

IL-13 and IFN-γ collaborate to activate the suppressive metabolic pathways in tumor-induced CD11b+ cells. Findings in KO mice and experiments with blocking mAbs indicate that MSCs can integrate the signals received from IL-13 and IFN-γ to activate their suppressive pathways. We evaluated whether antagonist cytokines such as IL-13 and IFN-γ could have a synergistic or additive effect on MSCs. Tumor-induced CD11b+ splenocytes cultured in vitro progressively lack the expression of IL-4Rα+ as a consequence of the autocrine release and binding of IL-13 to this receptor (Figure 7A). Receptor loss, in fact, was delayed by addition of an IL-13 blocking mAb (Figure 7A). Inhibition of IL-4Rα downregulation was also achieved with the addition of IFN-γ to CD11b+ cell cultures. This effect was likely independent from an IFN-γ–mediated inhibition of IL-13 release, since the combination of IFN-γ and IL-13 blocking

KO mice and control littermates. The transfer of CD8+ T lymphocytes purified from mice immunized with γ-irradiated C26-GM cells marginally affected the tumor development in control mice but completely prevented the tumor growth in LysM[Cre]IL-4R[−/flox] mice (Figure 6A). Moreover, CD8+ T lymphocytes staining with a tetramer loaded with AH1 peptide (AH1-TET), one of the major C26-GM–associated antigens (10, 37), were increased in the blood of LysM[Cre]IL-4R[−flox] but not of control mice after adoptive transfer to tumor-bearing hosts (Figure 6B). This difference was even more evident when the total number of AH1-TET+ cells in the blood was considered, because of a reduction in the number of CD3+CD8+ T cells circulating in the blood of control mice (Figure 6C). We estimated the number of circulating tumor-specific CD8+ T cells, taking into account the published figures of circulating white
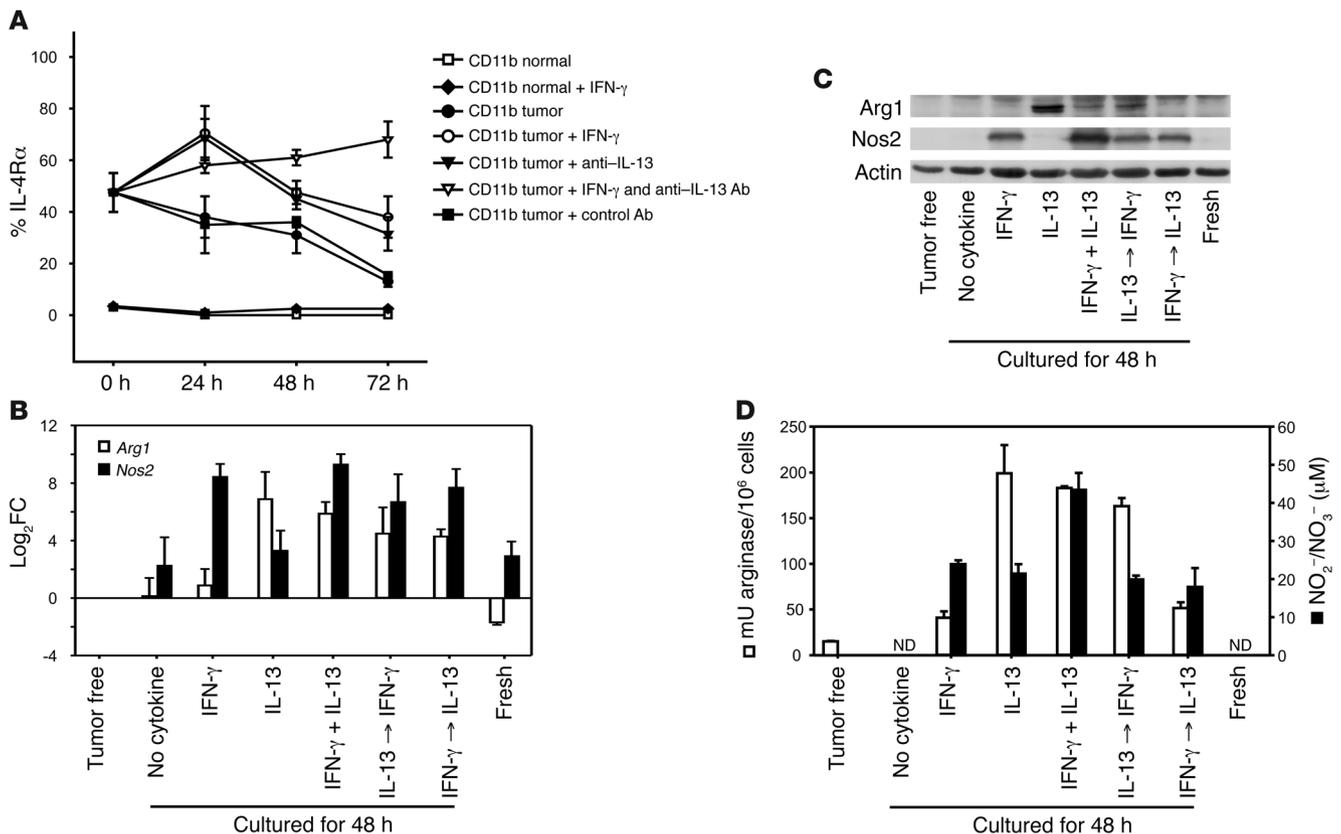
Figure 7

IFN-γ and IL-13 cooperate in the activation of immunosuppressive pathways. (**A**) Kinetics of IL-4Rα expression at the cell surface of tumor-induced CD11b^{+} splenocytes. CD11b^{+} splenocytes from tumor-free (normal) or tumor-bearing mice (tumor) were incubated for 72 hours alone, with IFN-γ, with a neutralizing antibody against mouse IL-13, or with both. Isotype-matched antibodies were included as negative controls. IL-4Rα protein expression on the cell surface was analyzed at various time points by flow cytofluorimetry and reported as the mean percentage of positive cells ± SEM of 3 separate determinations. Differences between diverging kinetics values were statistically significant ($P < 0.05$). (**B**–**D**) Effect of CD11b^{+} cell exposure to IL-13 and IFN-γ. CD11b^{+} cells were sorted from the spleens of tumor-free and tumor-bearing mice. These last cells were analyzed immediately (Fresh) or cultured for 48 hours in medium alone (No cytokine) or in the presence of IFN-γ, IL-13, or both. Some samples were treated either with IFN-γ for 24 hours followed by addition of IL-13 for a further 24 hours (IFN-γ → IL-13) or with the inverse cytokine combination (IL-13 → IFN-γ). Cells were then analyzed for expression of *Arg1* and *Nos2* mRNA by real-time PCR (**B**), for Arg1 and Nos2 protein levels by Western blotting (**C**), and for relative enzyme activity (**D**). Log$_2$FC is the log-transformed gene expression value of the target gene, normalized to an endogenous reference and relative to a calibrator sample. ND, not done. Data for real-time-PCR, Western blot, and enzyme activity are from the same experiment representative of 3.

mAbs had a synergistic effect on IL-4Rα persistence (Figure 7A). Moreover, IFN-γ did not modify the amount of secreted IL-13 monitored by ELISA in the supernatant of CD11b^{+} cells during the in vitro culture (data not shown). The IL-4Rα was negligible in CD11b^{+} cells enriched from the spleen of tumor-free mice, and IFN-γ did not affect its expression levels (Figure 7A).

To address further the basis of IL-13 and IFN-γ cooperation in MSC suppression, we cultured tumor-induced CD11b^{+} splenocytes for 48 hours in complete medium with or without IFN-γ or IL-13. We examined the effects different combinations of IFN-γ and IL-13 would have on the expression of the enzymes Arg1 and Nos2, which are the key molecules responsible for MSC-dependent suppression of T cells (Figure 7, B and C).

Fresh and cultured CD11b^{+} splenocytes isolated from tumor-bearing mice showed *Nos2* mRNA upregulation, while the relative proteins remained below the detection limits of the immunoblot (Figure 7, B and C). *Arg1*, which is strongly upregulated after 24

hours in cultured CD11b^{+} cells (Table 1 and unpublished data), returned to basal levels after 48-hour culture (Figure 7B). As expected, when each cytokine was added separately, IFN-γ caused preferential expression of Nos2, whereas IL-13 upregulated Arg1. Importantly, when the cytokines were added simultaneously or in the sequence IL-13 followed by IFN-γ and vice versa, the transcripts, proteins, and functional activities of the 2 enzymes were upregulated rather than inhibited (Figure 7, B and C). The cooperation between IL-13 and IFN-γ, inducing concomitant expression and activation of Arg1 and Nos2, thus identifies a unique property of MSCs. In fact, in inflammatory peritoneal macrophages, IL-13 pretreatment was shown to suppress Nos2 protein (but not mRNA) expression and activity induced by IFN-γ and LPS (39).

Intratumoral CD11b^{+} cells are potent immune suppressors. It has been suggested that tumor-infiltrating myeloid suppressors are different from circulating precursors from which they derive in various respects: they are promptly suppressive, not requiring in
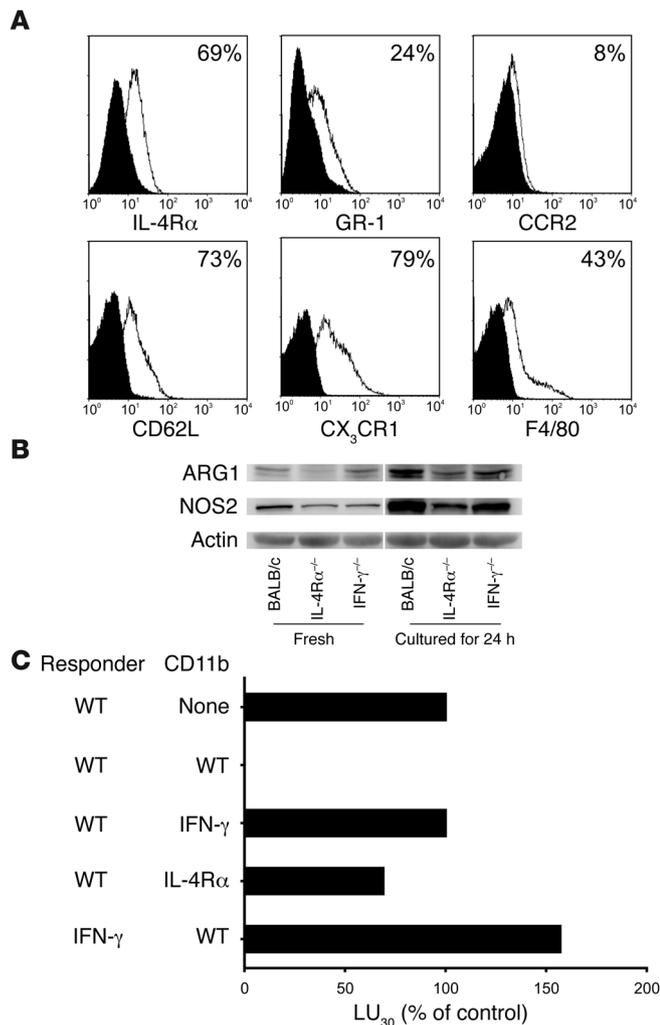
A

B

C

Figure 8
Phenotypic and functional characterization of CD11b^{+} cells infiltrating the tumor. (**A**) CD11b^{+} cells were separated from the disaggregated nodules of C26-GM tumor and stained with the indicated mAbs. (**B**) ARG1 and NOS2 protein expression level in CD11b^{+} cells isolated from tumors of WT, IL-4Rα^{−/−}, and IFN-γ^{−/−} BALB/c mice, analyzed immediately (Fresh) and after 24 hours of culture in standard medium. (**C**) Cytotoxicity of WT and IFN-γ^{−/−} BALB/c splenocytes (Responder), stimulated with an equal number of γ-irradiated C57BL/6 splenocytes and cocultured without (None) or with CD11b^{+} cells sorted from tumors of WT, IL-4Rα^{−/−}, and IFN-γ^{−/−} BALB/c mice. Data are the mean of 2 separate experiments.

CD11b^{+} cells isolated from tumor-bearing IL-4Rα^{−/−} mice. Interestingly, reduction in the level of Nos2 protein was detected in both IFN-γ^{−/−} and IL-4Rα^{−/−} mice (Figure 8B). Despite the slight phenotypic differences described above, intratumoral CD11b^{+} cells behaved functionally as did the splenic counterpart isolated in tumor-bearing mice: in fact, suppression of alloreactive T cells required IFN-γ release by activated T cells, autocrine production of IFN-γ, and the activation of the IL-13/IL-4Rα signaling pathway in CD11b^{+} cells (Figure 8C).

Discussion
Chronic and smoldering inflammation increase the risk of neoplasia, and infectious agents are estimated to be involved in over 15% of the malignancies worldwide (41). A complex and partially known pathogen-host interaction can alter gene pathways controlling cell homeostasis or exert an indirect tumor-favoring activity on nearby untransformed host cells. An inflamed stroma can promote the development of adjoining cancers from epithelial cells (41), and immunosuppression might be necessary to counteract the silent but constant "immunosurveillance," the process by which the immune system protects hosts against tumor development and selects tumors with reduced immunogenicity (42).

Our study offers a different view of the interplay between inflammation and cancer. Tumors themselves can sustain an inflammatory state and recruit a unique population of inflammatory and immunosuppressive monocytes. We assign a functional marker to these cells, which is critical for the in vivo inhibitory properties, i.e., the α chain common to the IL-4 and IL-13 receptor; moreover, we describe their capacity to spontaneously release IL-13 and IFN-γ. Their phenotype is consistent with the recently described inflammatory monocytes circulating in the blood of normal mice (34, 35). To become fully suppressive these circulating inflammatory cells must (a) be activated by the IFN-γ production of antigen-stimulated T lymphocytes; (b) release their own IFN-γ; and (c) be responsive to IL-13. Cooperation between these 2 cytokines leads to the activation of Arg1 and Nos2 enzymes that ultimately mediate the dysfunctional responses of T cells (Figure 9). These results bring together a plethora of conflicting data attributing a prevalence to either the IFN-γ/NOS2 or the IL-4,IL-13/ARG axis in the suppression of the immune response in tumor-bearing hosts (reviewed in refs. 21, 43). Tumor-induced suppression by myeloid cells is a multistep process, and interference with each single step might be sufficient to restore immune reactivity compromised in tumor-bearing hosts. Moreover, our data suggest a reevaluation of the concept that tumor-infiltrating macrophages are alternatively activated, since they require the same combination of Th1- and Th2-type cytokines necessary to trigger immunosuppressive pathways in circulating monocytes (Figure 9).

vitro culture, and express enzymatically active Arg1 and Nos2 that are critical for the immunosuppressive pathway since pharmacological interference with both enzymes restores the T lymphocyte response (10, 14). We thus evaluated phenotypic and functional properties of tumor-infiltrating myeloid suppressors. CD11b^{+} cells isolated from the cellular infiltrate of C26-GM nodules were potent immune suppressors, since they completely prevented cell division of clonotypic CL4 cells (Figure 1B) stimulated by the cognate antigen and induced their extensive cell death by apoptosis (Supplemental Figure 2). As described by others, CD11b^{+} cells are mostly Gr-1^{−} and express a variable amount of the marker F4/80 (Figure 8A), suggesting a differentiation toward mature macrophages (14, 35, 40). However, a relevant fraction of tumor-associated CD11b^{+} cells possessed the IL-4Rα (69% ± 1.59%, $n = 3$). Interestingly, whereas CD62L expression and CX$_3$CR1 expression were similar to those observed in splenic CD11b^{+} cells, the CCR2 was absent (Figure 8A), a likely consequence of the local production of the chemokine CCL2, detected by RT-PCR in the very same intratumoral CD11b^{+} cells (data not shown).

Tumor-infiltrating CD11b^{+} cells constitutively expressed Arg1 and Nos2 protein, and this expression was further enhanced by the in vitro culture in standard medium. As expected, a reduction of Arg1 protein levels was observed in fresh and cultured

Model of MSC activation

Figure 9
Mechanisms of MSC-dependent suppression. In the "triggering phase," T lymphocytes activated by exposure to the antigen release IFN-γ that, possibly in conjunction with a not yet identified membrane signal, activates inflammatory monocyte precursors. Whereas in resting condition this would result in induction of classically activated macrophages, monocytes conditioned by tumors show a different program because of the expression of IL-4Rα and the ability to release both IL-13 and IFN-γ. The IFN-γ production, initially sustained by activated T lymphocytes, is subsequently amplified by the cytokine released from activated monocytes. IFN-γ allows the prolonged expression and signaling of IL-4Rα after engagement by IL-13 released via an autocrine circuit. During the "amplification phase," the cytokines are thus able to maintain a prolonged activation of the enzymes NOS and ARG, which ultimately originate the immunosuppressive mediators acting on the CD8+ T cells. This model supports the view that a prolonged stimulation of MSCs is necessary to mediate a full inhibition of CD8+ T cells and explains why T cells can initially proliferate in the presence of spleen-derived MSCs. On the other hand, ARG and NOS are constitutively activated in tumor-infiltrating MSCs, which account for the prompt immunosuppression provided by these cells (Figure 1).

MSCs at the tumor site are similar but not identical to the cells circulating in the blood, which likely represent their precursors. CD11+Gr-1+CCR2+CX3CR1low cells are the first identifiable step, circulating in the blood, along monocyte/macrophage lineage differentiation and retain the ability to originate both macrophages and dendritic cells when exposed to the proper signals (reviewed in ref. 35). We suspect that, once at the tumor site, these cells receive further differentiation/maturation signals. Tumor-infiltrating MSCs are probably more similar to mature macrophages, as shown by their F4/80+Gr-1lowCCR2−CX3CR1+ phenotype, but are unable to mature toward stages compatible with an APC function. It has been shown, in fact, that intratumoral myeloid cells have a maturation defect, likely induced by the activation of the STAT3 pathway within the tumor microenvironment (reviewed in ref. 16).

GM-CSF appears to be one of the principal mediators of tumor-induced MSC recruitment and activation (43). Similarly to many cytokines, GM-CSF possesses a dual nature as immune modulator. GM-CSF production by many human and mouse tumor cell lines (2) supports its role as an immunosuppressive cytokine. On the other hand, experimental data have extensively proven that tumor cells engineered in vitro to produce GM-CSF are very effective cancer vaccines (44). Recent studies suggest that the amount and timing of GM-CSF could be critical to regulate the balance between adjuvant activity and immune suppression. A vaccine using a bystander tumor cell line producing high levels of GM-CSF admixed with autologous tumor cells at different ratios demonstrated that high doses of GM-CSF impaired the development of an effective antitumor immune response through the induction of immunosuppressive CD11b+ cells (45). Many cells activated during the inflammatory process (macrophages, T and NK cells) release GM-CSF, and it has been advanced that this cytokine might activate a feedback circuit restraining the excessive activation of the immune system (21, 43). Since administration of recombinant mouse GM-CSF is sufficient to recruit immunosuppressive CD11b+IL-4Rα+ cells in the blood and secondary lymphoid organs (I. Marigo et al., unpublished observations), these cells are good candidates for GM-CSF–dependent, immune-restraining functions.

The absence of any effect of the selective ablation of IL-4Rα in MSCs on the tumor growth in mice that did not receive adoptive transfer of tumor-specific CD8+ T cells (Figure 6A) suggests that the endogenous T cell response is not primed sufficiently, even in the absence of functional MSCs. This assumption is confirmed by the lack of AH1-TET+ cell expansion in the blood of KO mice (Figure 6B). We have already shown in this tumor model that growing cells are not immunogenic when compared with γ-irradiated cells (10, 37).

CD11b+IL-4Rα+ cells are normally present at very low numbers in normal, tumor-free mice and do not appear to be immunosuppressive. Recent observations, however, suggest that these few cells can respond to exogenously provided IL-13 and acquire suppressive activity. Expansion of the MSC pool, in fact, is not always required for tumor-induced inhibition of T cell responses. MSCs are part of a circuit that negatively affects tumor immunity and might involve participation of NKT cells. In a transformed fibrosarcoma model that grows, spontaneously regresses, and then recurs, Berzofsky and colleagues demonstrated that tumor-activated NKT cells primed CD11b+Gr-1+ cells to suppress tumor-specific CTLs. In this model, tumor recurrence was prevented by depletion of CD4+ NKT cells that mediated CD8+ T cell suppression by releasing IL-13, which in turn acted through the IL-4Rα/STAT6 pathway (33). The authors demonstrated that IL-13 activated CD11b+Gr-1+ cells, which directly suppressed CD8+ CTLs (9). Tumor recurrence was prevented by administration of an anti–Gr-1 antibody in vivo. Since this pathway is activated very early after tumor implantation in normal mice, these findings suggest that the few IL-4Rα+ cells present under steady state require activation by exogenous IL-13. It is not clear, at the moment, whether other tumor-released factors can prime these cells and make them more responsive to IL-13. In this regard, in the A20 mouse lymphoma model, tumor progression is accompanied not by an increase in the number of splenic CD11b+ cells but rather by their IL-4Rα upregulation (P. Serafini, unpublished observations).

Our study opens new scenarios for the therapeutic correction of tumor-induced immune dysfunctions. As shown in Figure 5C, the blockade of both IFN-γ and IL-13 has an additive/synergistic effect that could be therapeutically explored. It is clear, in fact, that the interference with the IL-13 signaling pathway, proposed by other studies (33), might not be as effective as the combined inhibition of the 2 cytokines in the presence of advanced disease and/or in different tumor types. The validity of a combined inhibition is

further strengthened by our recent demonstration that only drugs affecting both ARG and NOS in vivo could enhance the antitumor activity of recombinant cancer vaccines in mouse tumor models and rescue the dysfunctional tumor-infiltrating T lymphocytes in human prostate cancers (10, 46).

Methods

Cell lines. CT26 is a carcinogen-induced, undifferentiated colon carcinoma, and 4T1 is a mouse mammary adenocarcinoma cell line; both are derived from BALB/c mice (H-2^d). The MBL-2 and EL-4 lymphomas and MCA203, a fibrosarcoma induced by 3-methylcholanthrene, are derived from C57BL/6 mice (H-2^b). The C26-GM cell line was derived from the C26 colon carcinoma (H-2^d) genetically modified to release GM-CSF. Briefly, GM-CSF cDNA was cloned into the LXSN retroviral vector, as previously described, and used to infect C26 cells (22). C26-GM cells used in this study produced GM-CSF at levels of 10–15 ng/ml from 10^6 cells in 48 hours. These cell lines were grown in DMEM (Invitrogen) or RPMI 1640 (Euroclone) supplemented with 2 mM L-glutamine, 10 mM HEPES, 20 μM 2-mercaptoethanol, 150 U/ml streptomycin, 200 U/ml penicillin, and 10% heat-inactivated FBS (Invitrogen).

Mice. Eight-week-old C57BL/6 (H-2^b) and BALB/c (H-2^d) mice were purchased from Harlan. IFN-γ$^{-/-}$ (*Ifn^{tm1Ts}*) and IL-4$^{-/-}$ (*Il4^{tm2Nnt}*) mice, both on BALB/c background, were purchased from The Jackson Laboratory. CD1$^{-/-}$ (*Cd1^{tm1Gru}*) BALB/c mice were kindly provided by Luc Van Kaer (Vanderbilt University, Nashville, Tennessee, USA). IL-4Rα$^{-/-}$ (*Il4ra^{tm1Sz}*) BALB/c mice were purchased from Taconic. Common γ (γc)/Rag2–double KO (*Rag2$^{-/-}$γc$^{-/-}$*) BALB/c mice were a gift from the Central Institute for Experimental Animals, Kawasaki, Japan. Transgenic mice expressing an α/β TCR specific for amino acids 512–520 from HA presented by K^d (CL4 mice) were a gift from L. Sherman (The Scripps Research Institute, La Jolla, California, USA). In our experiments, CL4 mice congenic for the Thy1.1 allele were used, and the Thy1.1$^+$CD8$^+$ cells were all positive for the clonotypic T cell receptor. LysM^{Cre}IL-4Rα$^{-/flox}$ mice were engineered with a deleted (IL-4Rα$^{-/-}$ mice) and a *loxP*-flanked IL-4Rα allele (IL-4Rα$^{flox/flox}$ mice) and Cre-recombinase expression under control of the regulatory region for the lysozyme M gene (LysM^{Cre} mice), thereby restricting Cre-mediated *loxP* recombination to only macrophages and neutrophils (36). Mouse strains were either generated using BALB/c ES cells or backcrossed to BALB/c for at least 9 generations before intercrossing. IL-4Rα$^{-/flox}$ littermates, behaving like BALB/c WT mice, were used as controls in experiments. Procedures involving animals and their care conformed to institutional guidelines that comply with national and international laws and policies. Animal care and experiments were approved by the institutional review board of Istituto Oncologico Veneto. Mice were inoculated s.c. on the left flank with tumor cells, and tumor growth was monitored every 2 days by caliper measurement.

Cytokines, mAbs, and synthetic peptides. Mouse GM-CSF, IL-13 (used at a final concentration of 33 ng/ml), and IFN-γ (25 ng/ml, final concentration) were purchased from PeproTech. The following antibodies were used for flow cytometric staining: rat anti–mouse CD124–PE (IL-4Rα) and the control rat IgG$_{2a}$–PE (BD Biosciences — Pharmingen); rat anti–mouse CD11b–PE, biotin-conjugated rat anti–mouse F4/80, and the control rat IgG$_{2a}$–PE (CALTAG Laboratories); biotin-conjugated rat anti–mouse CD62L (BD Biosciences — Pharmingen); rat anti–mouse Gr-1–FITC (Immunokontact) and isotype control rat IgG$_{2b}$–FITC (CALTAG Laboratories); CX$_3$CR1-Fc (a gift from Millennium) and Cy5–goat anti-human IgG (The Jackson Laboratory); purified goat polyclonal IgG anti-CCR2 (CKR-2B) and isotype control normal goat IgG (Santa Cruz Biotechnology Inc.); FITC-conjugated rat anti–mouse IFN-γ (BD Biosciences — Pharmingen) and biotin-conjugated rat anti–mouse IL-13 (BioSource International). Neutralizing mAb goat anti–mouse IL-13 (30 μg/ml; R&D Systems), neutralizing mAb rat

anti–mouse IFN-γ R4-6A2 (30 μg/ml, HB370; ATCC), and normal goat or rat IgG (30 μg/ml; R&D Systems) were added to the culture at the beginning and after 72 hours of incubation.

The MHC class I L^d-restricted HA$_{512-520}$ peptide (IYSTVASSL) was synthesized by the Johns Hopkins Synthesis Facility (Baltimore, Maryland, USA). The peptide was greater than 95% pure, as indicated by HPLC. Lyophilized peptide was dissolved in DMSO (Sigma-Aldrich), and stored at –80°C before use.

Cell isolation and culture. Tumor-bearing or tumor-free mice were sacrificed, and their spleens were harvested under sterile conditions. Single-cell suspensions were prepared, and cells were isolated from spleen using magnetic microbeads conjugated with monoclonal rat anti–mouse/human CD11b (M1/70.15.11.5), or with rat anti–mouse CD8 (Miltenyi Biotec). Cells were washed with cold buffer to remove unbound antibody and were isolated on VarioMACS columns (Miltenyi Biotec) according to the manufacturer's instructions. Purity of cell populations was evaluated by flow cytometry and exceeded 90%. To separate the CD11b$^+$Gr-1$^+$ and CD11b$^+$Gr-1$^-$ cells, splenocytes were resuspended in MACS buffer and incubated with biotinylated anti-Gr-1 for 15 minutes at 4°C. Cells were washed with cold buffer to remove unbound beads, and then incubated with streptavidin microbeads for 15 minutes at 4°C. Gr-1$^+$ cells were all CD11b$^+$. The Gr-1$^-$ fraction was further incubated with anti–mouse/human CD11b microbeads to isolate the cells that constituted the CD11b$^+$Gr-1$^-$ fraction. In some experiments, CD11b$^+$ cells were cultured for 24–48 hours in complete medium at a density of 5×10^5 to 5×10^6 cells/ml in 24-well flat-bottom plates (BD Biosciences).

Evaluation of CTL response. To generate alloreactive CTLs, splenocytes (3×10^6) from BALB/c mice were incubated with 3×10^6 γ-irradiated C57BL/6 splenocytes. After 5 days, cultures were tested for ability to lyse allogenic target (MBL-2) in a 5-hour ^{51}Cr-release assay using 2×10^3 target cells previously labeled with 100 μCi of Na$_2$^{51}CrO$_4$ for 60 minutes. The percentage of specific lysis was calculated from triplicate samples as follows: (experimental cpm – spontaneous cpm)/(maximal cpm – spontaneous cpm) × 100. Lytic units (LU) were calculated as the number of cells giving 30% specific lysis of 2,000 allogeneic target cells (MBL-2 cells) per 10^6 effector cells (LU$_{30}$/10^6 cells). When present, the percent nonspecific lysis of CT26 control targets was subtracted from that obtained with MBL-2 target cells. The number of LU$_{30}$/10^6 cells was then used to calculate LU$_{30}$ per culture from the number of viable cells recovered in the cultures. The percentage of LU$_{30}$ was calculated as follows: LU$_{30}$ of experimental group/LU$_{30}$ of control group × 100. Data are thus expressed as a percentage of LU$_{30}$ measured in cultures containing the third-party MSCs and in control cultures set up in the absence of added third-party cells.

^{3}H-TdR incorporation. CD8$^+$ T cells (2×10^5 cells per well) were cultured in 96-well flat-bottom plates (BD Biosciences) and stimulated with 3 μg/ml anti-CD3 (2C11; ATCC) and 2 μg/ml anti-CD28 (clone 37.5; ATCC). CD11b$^+$ cells were added to the culture so as to constitute 20% of the total cells. After 2 days of incubation, cultures were pulsed with 1 μCi/well ^{3}H-TdR (PerkinElmer) for 18 hours, and ^{3}H-TdR incorporation was measured by scintillation counting.

Adoptive transfer of CD8$^+$ T lymphocytes. Single-cell suspensions were prepared from the spleens harvested from transgenic donors. Cells were washed in sterile HBSS (Invitrogen), and 3×10^6 naive Thy1.1$^+$, CD8$^+$ anti-HA TCR$^+$ T cells were injected into the tail veins of male BALB/c recipients (Thy1.2$^+$). Three days later, mice were primed by s.c. inoculation of 1×10^7 PFUs of HA-encoding vaccinia virus prepared as previously described (47). For in vitro experiments, spleens containing primed CL4 cells were harvested 1 week later. For adoptive transfer studies with LysM^{Cre}IL-4R$^{-/flox}$, IFN-γ$^{-/-}$, and BALB/c mice, the donor mice (BALB/c, either WT or IFN-γ$^{-/-}$) were immunized s.c. with γ-irradiated C26-GM

cells, and, after 14 days, 5×10^6 CD8$^+$ T cells enriched from the spleen and lymph nodes (>95% pure) were injected i.v. into LysM^{Cre}IL-4R$\alpha^{-/flox}$ mice, IFN-$\gamma^{-/-}$ mice, and control littermates.

Synthesis of MHC/peptide tetrameric complexes. The MHC class I L^d-restricted peptide corresponding to amino acids 423–431 of gp70 (AH1 peptide) was synthesized by automatic solid-phase procedures (37). Peptide corresponding to amino acids 876–884 of β-gal protein was synthesized and purified by Technogen. PE-labeled H-2 peptide tetramers were produced by mixture of the biotinylated complexes with Extravidin-PE (Sigma-Aldrich) and were validated by staining of CTL clones with the appropriate specificity, as previously reported (37).

CFSE labeling and proliferation assay. Splenocytes were derived either from naive Thy1.1$^+$ CL4 mice or from Thy1.2$^+$ mice that had received Thy1.1$^+$, CL4 T cells and subsequently primed with HA-encoding vaccinia virus. Splenocytes were washed twice with PBS and resuspended at 10^7 cells/ml in PBS/1% BSA, 1 μM CFSE (Invitrogen) for 10 minutes at 37°C. The labeling was stopped by washing twice with cold PBS/BSA. CFSE-labeled splenocytes (10^6) containing HA-specific CD8$^+$ T cells (10%–12% splenocytes for naive and 1%–2% splenocytes for HA-primed, respectively) were then stimulated for 60 hours in 96-well flat-bottom plates (BD Biosciences) with HA$_{512-520}$ peptide (5 μM). Cells were stained with rat anti–mouse CD8–PE and mouse anti-Thy1.1–allophycocyanin (BD Biosciences — Pharmingen). A total of 100,000 events were collected for each sample on a FACSCalibur flow cytometer (BD), and the data were analyzed using FCS Express (version 2.0; DeNovo Software).

Flow cytometry analysis and cell sorting. CD11b$^+$ cells (10^5 per sample) were resuspended in 50 μl of FACS buffer (0.9% NaCl solution containing 2% BSA and 0.02% NaN$_3$, both from Sigma-Aldrich) with anti–mouse Fc-γ receptor 2.4G2 mAb ascites (HB-197; ATCC) for 10 minutes at room temperature to reduce the nonspecific staining. The samples were washed and resuspended in 50 μl of FACS buffer for staining with the proper amount of antibodies. After 30 minutes, the cells were washed, resuspended in FACS buffer, and analyzed with a FACSCalibur flow cytometer (BD). For flow cytometric analysis of antigen-specific intracellular IFN-γ and IL-13 production, the CD11b$^+$ cells were incubated with 1 μg/ml brefeldin A (Sigma-Aldrich) for 10 hours. Cells were washed, fixed, and permeabilized for 20 minutes at 4°C (Cytofix/Cytoperm Kit; BD Biosciences — Pharmingen) before staining with either anti–mouse IFN-γ or anti–mouse IL-13 mAbs. Data analysis was carried out using CellQuest software (BD). The CD11b$^+$IL-4Rα^+ cells were presorted with microbeads conjugated with monoclonal rat anti–mouse/human CD11b and then labeled with anti–mouse CD124–PE and sorted to obtain highly purified populations using a FACSVantage DiVa (BD) equipped with a 488-nm argon laser (Innova 305C-BD; Coherent), at a rate of 8,000–12,000 cells per second. The sorted populations used in each experiment were over 97% pure. Adequate controls regarding the cell viability were performed using light-scattered parameters and propidium iodide/annexin V staining. For the tetramer analysis, PBMCs were labeled with AH1 tetramer–PE (AH1-TET, 5 μg/ml) for 20 minutes at room temperature. Each sample was then stained at 4°C with rat anti–mouse CD8–TRI-COLOR (CTCD8α; CALTAG Laboratories) and with hamster anti–mouse CD3–FITC (clone 145-2C11; CALTAG Laboratories). After 30 minutes, the cells were washed, resuspended in FACS buffer, and analyzed with a FACSCalibur flow cytometer (BD). Every sample was also stained with the control β-gal–TET according to a previously described protocol (37).

ELISPOT assay. ELISPOT was performed using the Mouse IFN-γ ELISPOT Kit (BD Biosciences — Pharmingen) according to the manufacturer's instructions. The numbers of spots were evaluated using the KS plate reader and software.

Morphological study of CD11b$^+$IL-4Rα^+ and CD11b$^+$IL-4Rα^- cells. Freshly isolated CD11b$^+$IL-4Rα^+ and CD11b$^+$IL-4Rα^- cells were spun on slides,

fixed in 95% ethanol for 20 minutes, and stained with May-Grünwald-Giemsa stain or H&E for 3 or 2 minutes, respectively. Microphotographs were taken at ×40 magnification.

Total RNA purification and real-time PCR analysis. Total RNA was extracted by TRIzoL (Invitrogen) from CD11b$^+$ sorted cells according to the manufacturer's instructions with minor modifications. The quality and quantity of RNA samples were determined by Agilent RNA 6000 Nano Chip (Agilent Technologies). cDNA from purified total RNA was produced by M-MLV reverse transcriptase (Invitrogen) according to the manufacturer's protocol. Twenty nanograms of template cDNA was used in TaqMan real-time PCR (TaqMan Gene Expression Assay; 2 minutes at 50°C, 10 minutes at 95°C, 15 seconds at 95°C, 1 minute at 60°C, for 45 cycles) performed on an ABI PRISM 7700 (Applied Biosystems) using the following assays-on-demand (Applera Corp.): mitochondrial ribosomal protein L33 (*Mrpl33*); arginase 1 liver (*Arg1*); and NO synthase 2, inducible, macrophage (*Nos2*). Threshold cycle was manually determined, and the fold change in expression was calculated as described by Applied Biosystems User Bulletin no. 2.

Gene expression. Gene expression was analyzed by the Affymetrix mouse genome expression set 230A (U74A). Five micrograms of RNA sample was amplified to biotinylated antisense RNA as described in the Affymetrix GeneChip Expression Analysis Technical Manual. Briefly, 5 μg of total RNA was used to generate double-stranded cDNA (Invitrogen). Synthesis of biotin-labeled antisense RNA was performed using the BioArray HighYield RNA Transcript Labeling Kit (Enzo). All the prehybridization quality controls were performed with the Agilent 2100 bioanalyzer (Agilent Technologies). Affymetrix Microarray Suite (MAS) 5.0 was used for single-array and comparison analysis.

Western blot analysis. Cells were harvested by pipetting and washed twice with cold PBS, and 5×10^5 pelleted cells were disrupted for 15 minutes on ice in lysis buffer (50 mM HEPES, 150 mM NaCl, 5 mM EDTA, 1 mM NaOV$_4$, 0.5% Triton, 0.1 μg/μl pepstatin, 0.1 μg/μl antipain, 0.1 μg/μl aprotinin, 2 mM PMSF). Lysates were decanted at 3,000 relative centrifugal fields for 10 minutes at 4°C, 1 volume of Laemmli's buffer was added to the supernatant, and denaturation was carried out for 5 minutes at 100°C. Proteins were separated on a 10% denaturing SDS polyacrylamide gel and transferred on a PVDF membrane (Millipore) for 2 hours at 4°C. The membrane was saturated for 1 hour at room temperature in PBS/0.05% Tween-20 (PBS-T) supplemented with different concentrations of nonfat dried milk (Sigma-Aldrich): 5% for anti-ARG1, 3% for anti-NOS2, and 1% for anti-actin. Hybridizations of primary antibody were carried out as follows: mouse monoclonal anti-ARG1 (1:200; a kind gift from A.C. Ochoa, Louisiana State University, New Orleans, Louisiana, USA) for 1 hour at room temperature in blocking buffer; polyclonal rabbit anti-NOS2 (1:1,000; Santa Cruz Biotechnology Inc.) overnight at 4°C in PBS-T/3% BSA; and polyclonal rabbit anti-actin antibody (1:500; Sigma-Aldrich) for 1 hour at room temperature in PBS-T/3% BSA. Hybridizations with the HRP-conjugated secondary antibodies mouse anti-mouse IgG (Sigma-Aldrich) and donkey anti-rabbit IgG (Amersham Biosciences) were performed for 1 hour at room temperature. Proteins were detected on Hyperfilm (Amersham Biosciences) by SuperSignal West Pico Chemiluminescent (Pierce).

Enzyme activity. NO released in the cultures was measured by Griess reaction as the amount of NO$_3^-$ and NO$_2^-$ produced, using a nitrate/nitrite assay kit (Cayman Chemicals). ARG activity was measured in cell lysates as previously described (10), and 1 U of ARG was defined as the amount that catalyzes the formation of 1 μg of urea per minute.

Statistics. The Wilcoxon-Mann-Whitney U test was used to examine the null hypothesis of rank identity between 2 sets of data. All *P* values presented are 2-sided. A *P* value of 0.05 or less was considered significant.

1. Bronte, V., et al. 1998. Apoptotic death of CD8+ T lymphocytes after immunization: induction of a suppressive population of Mac-1+/Gr-1+ cells. *J. Immunol.* **161**:5313–5320.
2. Bronte, V., et al. 1999. Unopposed production of granulocyte-macrophage colony-stimulating factor by tumors inhibits CD8+ T cell responses by dysregulating antigen-presenting cell maturation. *J. Immunol.* **162**:5728–5737.
3. Kusmartsev, S., Nefedova, Y., Yoder, D., and Gabrilovich, D.I. 2004. Antigen-specific inhibition of CD8+ T cell response by immature myeloid cells in cancer is mediated by reactive oxygen species. *J. Immunol.* **172**:989–999.
4. Almand, B., et al. 2001. Increased production of immature myeloid cells in cancer patients: a mechanism of immunosuppression in cancer. *J. Immunol.* **166**:678–689.
5. Bronte, V., et al. 2000. Identification of a CD11b+/ Gr-1+/CD31+ myeloid progenitor capable of activating or suppressing CD8+ T cells. *Blood.* **96**:3838–3846.
6. Gabrilovich, D.I., Velders, M.P., Sotomayor, E.M., and Kast, W.M. 2001. Mechanism of immune dysfunction in cancer mediated by immature gr-1(+) myeloid cells. *J. Immunol.* **166**:5398–5406.
7. Salvadori, S., Martinelli, G., and Zier, K. 2000. Resection of solid tumors reverses T cell defects and restores protective immunity. *J. Immunol.* **164**:2214–2220.
8. Sinha, P., Clements, V.K., and Ostrand-Rosenberg, S. 2005. Reduction of myeloid-derived suppressor cells and induction of M1 macrophages facilitate the rejection of established metastatic disease. *J. Immunol.* **174**:636–645.
9. Terabe, M., et al. 2003. Transforming growth factor-beta production and myeloid cells are an effector mechanism through which CD1d-restricted T cells block cytotoxic T lymphocyte-mediated tumor immunosurveillance: abrogation prevents tumor recurrence. *J. Exp. Med.* **198**:1741–1752.
10. De Santo, C., et al. 2005. Nitroaspirin corrects immune dysfunction in tumor-bearing hosts and promotes tumor eradication by cancer vaccination. *Proc. Natl. Acad. Sci. U. S. A.* **102**:4185–4190.
11. Pekarek, L.A., Starr, B.A., Toledano, A.Y., and Schreiber, H. 1995. Inhibition of tumor growth by elimination of granulocytes. *J. Exp. Med.* **181**:435–440.
12. Serafini, P., et al. 2003. Derangement of immune responses by myeloid suppressor cells. *Cancer Immunol. Immunother.* **53**:64–72.
13. Yang, L., et al. 2004. Expansion of myeloid immune suppressor Gr+CD11b+ cells in tumor-bearing host directly promotes tumor angiogenesis. *Cancer Cell.* **6**:409–421.
14. Kusmartsev, S., and Gabrilovich, D.I. 2005. STAT1 signaling regulates tumor-associated macrophage-mediated T cell deletion. *J. Immunol.* **174**:4880–4891.
15. Young, M.R., Wright, M.A., Matthews, J.P., Malik, I., and Prechel, M. 1996. Suppression of T cell proliferation by tumor-induced granulocyte-macrophage progenitor cells producing transforming growth factor-beta and nitric oxide. *J. Immunol.* **156**:1916–1922.
16. Gabrilovich, D. 2004. Mechanisms and functional significance of tumour-induced dendritic-cell defects. *Nat. Rev. Immunol.* **4**:941–952.
17. Nefedova, Y., et al. 2004. Hyperactivation of STAT3 is involved in abnormal differentiation of dendritic cells in cancer. *J. Immunol.* **172**:464–474.
18. Takeda, K., Hatakeyama, K., Tsuchiya, Y., Rikiishi, H., and Kumagai, K. 1991. A correlation between GM-CSF gene expression and metastases in murine tumors. *Int. J. Cancer.* **47**:413–420.
19. Young, M.R., et al. 1997. Increased recurrence and metastasis in patients whose primary head and neck squamous cell carcinomas secreted granulocyte-macrophage colony-stimulating factor and contained CD34+ natural suppressor cells. *Int. J. Cancer.* **74**:69–74.
20. Pak, A.S., et al. 1995. Mechanisms of immune suppression in patients with head and neck cancer: presence of CD34+ cells which suppress immune functions within cancers that secrete granulocyte-macrophage colony-stimulating factor. *Clin. Cancer Res.* **1**:95–103.
21. Bronte, V., and Zanovello, P. 2005. Regulation of immune responses by L-arginine metabolism. *Nat. Rev. Immunol.* **5**:641–654.
22. Bronte, V., et al. 2003. IL-4-induced arginase 1 suppresses alloreactive T cells in tumor-bearing mice. *J. Immunol.* **170**:270–278.
23. Brito, C., et al. 1999. Peroxynitrite inhibits T lymphocyte activation and proliferation by promoting impairment of tyrosine phosphorylation and peroxynitrite-driven apoptotic death. *J. Immunol.* **162**:3356–3366.
24. Brys, L., et al. 2005. Reactive oxygen species and 12/15-lipoxygenase contribute to the antiproliferative capacity of alternatively activated myeloid cells elicited during helminth infection. *J. Immunol.* **174**:6095–6104.
25. Gordon, S. 2003. Alternative activation of macrophages. *Nat. Rev. Immunol.* **3**:23–35.
26. Mantovani, A., Sozzani, S., Locati, M., Allavena, P., and Sica, A. 2002. Macrophage polarization: tumor-associated macrophages as a paradigm for polarized M2 mononuclear phagocytes. *Trends Immunol.* **23**:549–555.
27. Apolloni, E., et al. 2000. Immortalized myeloid suppressor cells trigger apoptosis in antigen-activated T lymphocytes. *J. Immunol.* **165**:6723–6730.
28. Mazzoni, A., et al. 2002. Myeloid suppressor lines inhibit T cell responses by an NO-dependent mechanism. *J. Immunol.* **168**:689–695.
29. Loke, P., et al. 2002. IL-4 dependent alternatively-activated macrophages have a distinctive in vivo gene expression phenotype. *BMC Immunol.* **3**:7.
30. Xaus, J., et al. 1999. IFN-gamma up-regulates the A2B adenosine receptor expression in macrophages: a mechanism of macrophage deactivation. *J. Immunol.* **162**:3607–3614.
31. Kelly-Welch, A.E., Hanson, E.M., Boothby, M.R., and Keegan, A.D. 2003. Interleukin-4 and interleukin-13 signaling connections maps. *Science.* **300**:1527–1528.
32. Goldman, J.P., et al. 1998. Enhanced human cell engraftment in mice deficient in RAG2 and the common cytokine receptor gamma chain. *Br. J. Haematol.* **103**:335–342.
33. Terabe, M., et al. 2000. NKT cell-mediated repression of tumor immunosurveillance by IL-13 and the IL-4R-STAT6 pathway. *Nat. Immunol.* **1**:515–520.
34. Geissmann, F., Jung, S., and Littman, D.R. 2003. Blood monocytes consist of two principal subsets with distinct migratory properties. *Immunity.* **19**:71–82.
35. Gordon, S., and Taylor, P.R. 2005. Monocyte and macrophage heterogeneity. *Nat. Rev. Immunol.* **5**:953–964.
36. Herbert, D.R., et al. 2004. Alternative macrophage activation is essential for survival during schistosomiasis and downmodulates T helper 1 responses and immunopathology. *Immunity.* **20**:623–635.
37. Bronte, V., et al. 2003. Effective genetic vaccination with a widely shared endogenous retroviral tumor antigen requires CD40 stimulation during tumor rejection phase. *J. Immunol.* **171**:6396–6405.
38. Nemzek, J.A., Bolgos, G.L., Williams, B.A., and Remick, D.G. 2001. Differences in normal values for murine white blood cell counts and other hematological parameters based on sampling site. *Inflamm. Res.* **50**:523–527.
39. El-Gayar, S., Thuring-Nahler, H., Pfeilschifter, J., Rollinghoff, M., and Bogdan, C. 2003. Translational control of inducible nitric oxide synthase by IL-13 and arginine availability in inflammatory macrophages. *J. Immunol.* **171**:4561–4568.
40. Rodriguez, P.C., et al. 2004. Arginase I production in the tumor microenvironment by mature myeloid cells inhibits T-cell receptor expression and antigen-specific T-cell responses. *Cancer Res.* **64**:5839–5849.
41. Balkwill, F., Charles, K.A., and Mantovani, A. 2005. Smoldering and polarized inflammation in the initiation and promotion of malignant disease. *Cancer Cell.* **7**:211–217.
42. Dunn, G.P., Old, L.J., and Schreiber, R.D. 2004. The immunobiology of cancer immunosurveillance and immunoediting. *Immunity.* **21**:137–148.
43. Serafini, P., Borrello, I., and Bronte, V. 2006. Myeloid suppressor cells in cancer: recruitment, phenotype, properties, and mechanisms of immune suppression. *Semin. Cancer Biol.* **16**:53–65.
44. Mach, N., and Dranoff, G. 2000. Cytokine-secreting tumor cell vaccines. *Curr. Opin. Immunol.* **12**:571–575.
45. Serafini, P., et al. 2004. High-dose granulocyte-macrophage colony-stimulating factor-producing vaccines impair the immune response through the recruitment of myeloid suppressor cells. *Cancer Res.* **64**:6337–6343.
46. Bronte, V., et al. 2005. Boosting anti-tumor responses of T lymphocytes infiltrating human prostate cancers. *J. Exp. Med.* **201**:1257–1268.
47. Staveley-O'Carroll, K., et al. 1998. Induction of antigen-specific T cell anergy: an early event in the course of tumor progression. *Proc. Natl. Acad. Sci. U. S. A.* **95**:1178–1183.